of opaque materials can give rise to a range of absorption band depths similar to the range observed (*14*).

As a final possibility for interpreting the observed range of spectral properties spanning the divide between S asteroids and OC meteorites, we would suggest that asteroids in the observed size range have the most diverse range of ages of any asteroid population sampled to date. Because significant collisions occur much more frequently for small objects, "young" fragments or "fresh" surfaces are most likely to be found among small asteroids (*19*). However, because collisions are a stochastic process, the sampled population will contain a wide range of surface ages. If a time-dependent weathering process (*7*) is active, as has been proposed to explain surface variations measured in Galileo spacecraft images of 243 Ida (*20*), asteroids most closely resembling OC meteorites would be those with the youngest surfaces. For this scenario, a wide range of surface ages could give rise to a continuum of spectral properties, such as we have observed.

REFERENCES AND NOTES

1. H. Y. McSween, *Meteorites and Their Source Bodies* (Cambridge Univ. Press, New York, 1987).
2. We define near-Earth asteroids on the basis of their orbital characteristics. For this work, we specifically refer to asteroids categorized as Aten, Apollo, and Amor objects. Aten and Apollo asteroids have orbits that cross the orbit of Earth. Amor asteroids approach within 0.3 astronomical unit of Earth's orbit.
3. G. W. Wetherill, *Philos. Trans. R. Soc. London Ser. A* **323**, 323 (1987); J. Wisdom, *Icarus* **56**, 51 (1983); *Nature* **315**, 731 (1985); R. P. Binzel, S. Xu, S. J. Bus, E. Bowell, *Science* **257**, 779 (1992).
4. D. J. Tholen and M. A. Barucci, in *Asteroids II*, R. P. Binzel, T. Gehrels, M. S. Matthews, Eds. (Univ. of Arizona Press, Tucson, 1989), pp. 298–315.
5. L. A. McFadden, M. J. Gaffey, T. B. McCord, *Science* **229**, 160 (1985).
6. Asteroid 1862 Apollo is the only object currently assigned to the taxonomic class Q, which is the OC analog case we consider here. Two other potential OC-like asteroids have been reported, but both have spectra that differ from that of Apollo. Asteroid 6611 (1993 VW) is a near-Earth asteroid measured by M. Di Martino, A. Manara, and F. Migliorini [*Astron. Astrophys.* **302**, 609 (1995)]. A potential main-belt asteroid OC analog, 3628 Boznemcova, is discussed by R. P. Binzel *et al.* [*Science* **262**, 1541 (1993)]. Near-Earth asteroids found to have spectra revealing other spectral types (for example, C types) will be discussed elsewhere (R. P. Binzel *et al.*, in preparation).
7. C. M. Pieters, *Meteoritics* **19**, 290 (1984); G. W. Wetherill and C. R. Chapman, in *Meteorites and the Early Solar System*, J. F. Kerridge and M. S. Matthews, Eds. (Univ. of Arizona Press, Tucson, 1988), pp. 35–67; C. M. Pieters, E. M. Fischer, O. Rode, A. Basu, *J. Geophys. Res.* **98**, 20817 (1993).
8. J. F. Bell, D. R. Davis, W. K. Hartmann, M. J. Gaffey, in (*4*), pp. 921–945.
9. S. Xu, R. P. Binzel, T. H. Burbine, S. J. Bus, *Icarus* **115**, 1 (1995).
10. S-class asteroids display a diverse range of mineralogies. One subset, denoted as S(IV), appears to have a silicate mineralogy most analogous to OC meteorites [M. J. Gaffey *et al.*, *Icarus* **106**, 573 (1993)].
11. R. G. Burns, *Mineralogical Applications of Crystal Field Theory* (Cambridge Univ. Press, New York, ed. 2, 1983). The slope shortward of 0.7 μm results from the charge transfer $O \rightarrow Fe^{2+}$.
12. The taxonomic classification for 4 Vesta is V. Numerous small main-belt asteroids having the same classification appear to be related to Vesta (*13*). (A second related set of small asteroids related to Vesta, denoted the J class, have the same mismatch seen in Fig. 1A at 0.8 μm.) Asteroid 349 Dembowska is the only object currently assigned to taxonomic class R (*4*).
13. R. P. Binzel and S. Xu, *Science* **260**, 186 (1993).
14. M. J. Gaffey, J. F. Bell, D. P. Cruikshank, in (*4*), pp. 98–127.
15. M. J. Gaffey, T. H. Burbine, R. P. Binzel, *Meteoritics* **28**, 161 (1993).
16. M. J. Gaffey, *J. Geophys. Res.* **81**, 905 (1976). We account for the 0.025-μm wavelength calibration error in these data [as reported on p. 91 of M. J. Gaffey, *Icarus* **60**, 83 (1984)].
17. Notable exceptions in our data set are the two largest near-Earth asteroids, 433 Eros and 1036 Ganymede, which have estimated diameters of >20 and >50 km, respectively. Three other sampled objects, 1627 Ivar, 1866 Sisyphus, and 4954 Eric, may have diameters of >10 km. For the remaining 30 objects in our sample, the estimated mean diameter is 3 km. Because the bulk of our observations span such a narrow size range, the observed variations in band depth are not part of a diameter-dependent trend reported in (*10*).
18. M. J. Gaffey, *Lunar. Planet. Sci. Conf.* **XXVII**, 391 (1996).
19. D. R. Davis, S. J. Weidenschilling, P. Farinella, P. Paolicchi, R. P. Binzel, in (*4*), pp. 805–826.
20. C. R. Chapman *et al.*, *Nature* **374**, 783 (1995); C. R. Chapman, in preparation.
21. B. Zellner, D. J. Tholen, E. F. Tedesco, *Icarus* **61**, 355 (1985).
22. The dispersion within our spectrograph is about 25 Å per pixel. To achieve a higher signal-to-noise ratio for compact plotting in this report, we further binned our data in 10-pixel increments with the resulting points and error bars representing the weighted least squares average of each independent 10-pixel sample.
23. The following near-Earth asteroid spectra are presented in Fig. 3B: 433, 1036, 1620, 1627, 1864, 1866, 2062, 2063, 2102, 4179, 4954, 5143, 5626, 5660, 6053, 6489, 6455, 6569, 1989 VA, 1991 BB, 1991 VK, 1991 WA, 1991 XB, 1992 CC1, 1993 TQ2, 1993 UB, 1993 WD, 1993 XN2, 1994 AB1, 1994 AW1, 1994 EF2, 1994 TW1, 1995 BL2, 1995 WL8, and 1995 YA3.

24. Data reported here were obtained at the MDM Observatory. This work was supported by NASA grants NAGW1450, NAGW3901, and NASW5026 and by a National Science Foundation Presidential Young Investigator Award (R.P.B.). A grant from the Planetary Society provided additional access to the telescope essential for the success of this project. We thank B. G. Marsden, G. V. Williams, and E. L. G. Bowell for assistance with ephemerides for newly discovered objects and M. Gaffey and an anonymous referee for helpful reviews.

26 April 1996; accepted 21 June 1996

Arabidopsis AUX1 Gene: A Permease-Like Regulator of Root Gravitropism

Malcolm J. Bennett,* Alan Marchant, Haydn G. Green, Sean T. May, Sally P. Ward, Paul A. Millner, Amanda R. Walker, Burkhard Schulz,† Kenneth A. Feldmann

The plant hormone auxin regulates various developmental processes including root formation, vascular development, and gravitropism. Mutations within the *AUX1* gene confer an auxin-resistant root growth phenotype and abolish root gravitropic curvature. Polypeptide sequence similarity to amino acid permeases suggests that *AUX1* mediates the transport of an amino acid–like signaling molecule. Indole-3-acetic acid, the major form of auxin in higher plants, is structurally similar to tryptophan and is a likely substrate for the *AUX1* gene product. The cloned *AUX1* gene can restore the auxin-responsiveness of transgenic *aux1* roots. Spatially, *AUX1* is expressed in root apical tissues that regulate root gravitropic curvature.

Auxins regulate many aspects of plant growth and development (*1*). Indole-3-acetic acid (IAA), the major form of auxin in higher plants, is synthesized from an indole precursor of the tryptophan amino acid biosynthetic pathway within shoot apical tissues (*2*). IAA is then redistributed from the shoot apex to other tissues (*3*), where it influences many cellular processes, including elongation growth (*4*). Our knowledge of the cellular machinery that mediates the transport and perception of IAA is limited. Several auxin-binding proteins have been identified, including putative carriers and receptors (*5*), but their physiological importance remains unclear. Molecular genetic approaches in *Arabidopsis thaliana* have provided new opportunities to identify and characterize novel auxin signaling components (*6*). We selected root gravitropism as our genetic model for auxin signaling.

Roots use specialized gravity-sensing columella cells located in the root cap to monitor root orientation. After a gravistimulus, the columella cells direct actively growing

M. J. Bennett, A. Marchant, H. G. Green, S. T. May, S. P. Ward, Department of Biological Sciences, University of Warwick, Coventry, CV4 7AL, UK.
P. A. Millner, Department of Biochemistry and Molecular Biology, University of Leeds, Leeds, West Yorkshire, UK.
A. R. Walker, Department of Plant Sciences, University of Cambridge, Cambridge, UK.
B. Schulz and K. A. Feldmann, Department of Plant Sciences, University of Arizona, Tucson, AZ 85721, USA.

*To whom correspondence should be addressed. E-mail: bt@dna.bio.warwick.ac.uk
†Present address: Botany Institute, University of Cologne, 50931 Cologne, Germany.

tissues within the elongation zone to undergo differential growth, leading to correctional bending (*7*). IAA regulates gravity-induced root curvature by acting as an inhibitor of root cell elongation, but the mechanism of IAA action remains controversial (*7*). We used an *Agrobacterium*-mediated transferred DNA (T-DNA) tagging procedure in *Arabidopsis* (*8*) to isolate and characterize the *AUX1* gene, the product of which mediates the hormonal control of root gravitropism. The *AUX1* polypeptide exhibits sequence similarity to a family of plant and fungal amino acid permeases, suggesting that *AUX1* mediates the transport of an amino acid–like signaling molecule.

An agravitropic root mutant, *aux1-100*, allelic with the *aux1* mutation (*9*, *10*), was isolated from an *Arabidopsis* population mutagenized by T-DNA (*11*). The *aux1-100* mutant also exhibited an altered thigmotropic growth response similar to that described for the *aux1* allele *wav5* (*12*). The *aux1-100* mutation, like other *aux1* alleles (*9*, *10*), confers a reduced sensitivity to the exogenously applied synthetic auxin 2,4-D [(2,4-dichlorophenoxy)acetic acid] (*13*).

The T-DNA insert cosegregating with the recessive *aux1-100* phenotype (*14*) served as a molecular marker for the putative *AUX1* locus. A genomic DNA fragment bordering the *aux1-100* T-DNA insert was isolated by plasmid rescue (*15*, *16*) and used to obtain a homologous cosmid clone, 20-1-1 (*17*). Restriction fragment length polymorphism (RFLP) analysis (*18*), with an *Arabidopsis* recombinant-inbred mapping population and a probe derived from 20-1-1, verified the linkage between the T-DNA insert and the *AUX1* gene on chromosome 2.

We isolated cDNA clones encoded by a single gene from an *Arabidopsis* cDNA library with probes from 20-1-1 (*19*). The longest cDNA, 1988 base pairs (bp) in length, encoded a full-length transcript (*19*). Sequence analysis identified nine exons and eight introns within the transcribed gene (Fig. 1) (*20*). The first exon, although featuring a short open reading frame, encodes only 5′ untranslated sequence. Exons two through nine collectively contain a single large open reading frame. The lesions of four *aux1* alleles were identified within the gene sequence (Fig. 1) (*21*).

We confirmed the identity of the *AUX1* gene by performing complementation of the *aux1-7* allele. Two genomic fragments that encompassed the entire open reading frame and included either 0.5 or 3.5 kbp of the upstream promoter sequence (Fig. 1) were subcloned into an *Agrobacterium* binary vector and transformed into *aux1-7* plants (*22*). Among the progeny of six independent *aux1-7* transformants, either *AUX1* gene fragment could complement the aux-

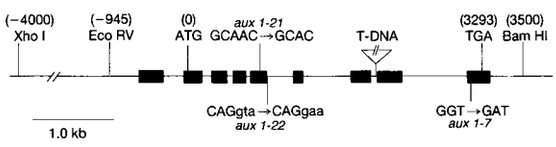

Fig. 1. Map of the *AUX1* gene. The structure of the *AUX1* gene is shown to scale, with black boxes representing exons. The positions of the initiation and termination codons of the predicted *AUX1* open reading frame are signified by ATG and TGA, respectively. The nucleotide sequence has been submitted to the EMBL database (*20*). Nucleotide sequence changes have been described for four *aux1* alleles (exon and intron sequences are in upper and lower case letters, respectively) as follows: A^{823} is deleted in *aux1-21*; a change from t^{939} to a^{939} in *aux1-22* alters the 5′ intron splice site consensus; there is a T-DNA insertion downstream of T^{2118} in *aux1-100*; and G^{3214} is changed to A^{3214} in *aux1-7*, resulting in a Gly^{459} to Asp^{459} missense amino acid substitution.

in-resistant *aux1* root-growth phenotype (Fig. 2). In contrast to the *aux1-7* phenotype, transgenic *aux1-7* roots expressing the cloned *AUX1* gene failed to elongate in the presence of the synthetic auxin 2,4-D at levels that normally inhibit wild-type root growth (Fig. 2). The *AUX1* transgene could also complement the root agravitropic and athigmotropic phenotypes (*23*).

The *AUX1* gene (Fig. 1) encodes a polypeptide of 485 amino acids with a predicted molecular mass of 54.1 kD. Database searches (*24*) with the *AUX1* amino acid sequence have identified similarity with several sequences from *Caenorhabditis elegans*, fungi, and plants (up to a smallest sum probability value of 2.5×10^{-8}). The sequences of known function share a common biochemical activity—amino acid transport—and comprise a family of sequence-related amino acid permeases from *Arabidopsis*, *Nicotiana*, and *Neurospora*, ranging from 470 to 493 amino acids in length (*25*). Both *AUX1* and the related *Arabidopsis AAP1* amino acid permease are predicted to contain between 10 and 12 transmembrane-spanning helices (*25*, *26*); when aligned, the *AUX1* and *AAP1* sequences demonstrate 21% identity and 48% similarity (*24*) and are essentially colinear along their entire length (Fig. 3). The similarities suggest that *AUX1* mediates the transport of an amino acid–like signaling molecule. The plant hormone IAA, which is structurally similar to the amino acid tryptophan, is a likely substrate. Plant cells mediate IAA uptake by cotransport of IAA anions and protons, whereas the efflux carrier transports IAA anions (*27*). Mechanistically, plant amino acid permeases function as proton-driven symporters (*28*), suggesting that *AUX1* may

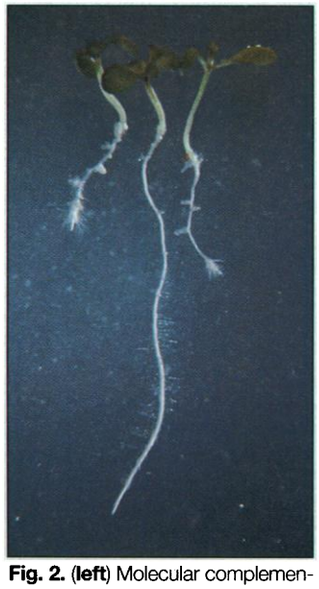

Fig. 2. (left) Molecular complementation of the *aux1-7* allele. A 7.5-kbp Xho I–Bam HI DNA fragment (see Fig. 1) encoding the *AUX1* gene was transformed into the *aux1-7* genetic background (*22*). Four-day-old wild-type, *aux1-7*, and transgenic *aux1-7* seedlings (left to right) were transferred to plates containing 5×10^{-7} M 2,4-D to assay auxin-mediated inhibition of root growth (*9*, *10*). The 7.5-kbp fragment restored a wild-type level of sensitivity to the synthetic auxin 2,4-D within the *aux1-7* genetic background. **Fig. 3. (right)** Amino acid sequence conservation between *AUX1* and the related amino acid permease AAP1 (*38*). The *Arabidopsis AUX1* (upper) and AAP1 (lower) sequences were optimally aligned. Residues are boxed to indicate amino acid identity (shaded) or functional conservation (open).

behave in an equivalent fashion to mediate proton-driven IAA uptake. Candidate IAA carriers have been identified with photoaffinity labeling techniques (*29*).

Auxin transport is often associated with gravitropism, particularly because inhibitors of auxin transport can abolish gravitropic bending (*30*). Two auxin transport streams have been identified in roots (*31*): an acropetal IAA transport stream associated with the central root tissues and a basipetal IAA transport stream localized to the epidermal tissue. Hasenstein and Evans (*32*) proposed that root gravitropic curvature is mediated by the asymmetric redistribution of IAA during basipetal transport away from the root tip to the cells of the elongation zone. Using a whole-mount in situ hybridization technique (*33*), we showed that *AUX1* expression is associated with the root apical tissues that control the root gravitropic response (Fig. 4). Furthermore, we observed that *AUX1* is expressed predominantly within root epidermal cells (*34*), thus underlining the close association between *AUX1* expression and basipetal auxin transport.

The relative importance of asymmetric changes in auxin concentration compared with tissue sensitivity during gravitropic curvature remains unclear (*7*). Apparent asymmetric tissue sensitivity may in fact reflect differential rates of IAA uptake by elongating cells on opposite sides of a gravistimulated organ. Regulating auxin uptake would thus be important, a view supported by recent studies in maize in which intracellular auxin concentration and growth rate were correlated (*35*). Experiments designed to block the auxin efflux carrier in roots result in reduced rates of growth (*30*), perhaps reflecting intracellular auxin accumulation. In contrast, inhibition of auxin uptake would deplete intracellular auxin levels, thus increasing the rate of root growth. The identical phenotype of the *aux1* mutant (*36*) provides further evidence that *AUX1* functions in IAA uptake. Permease-based signaling mechanisms may prove to be of general importance to other auxin-regulated growth processes, particularly because *AUX1* belongs to a family of closely related sequences in *Arabidopsis* that are likely to have related biochemical activities (*37*).

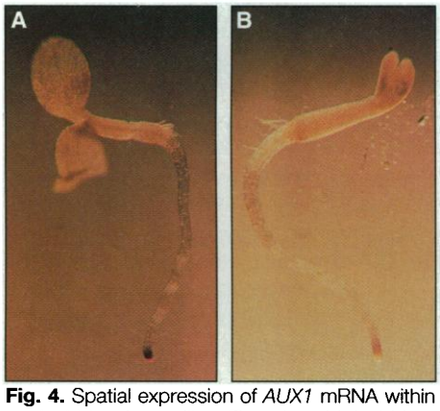

Fig. 4. Spatial expression of *AUX1* mRNA within an *Arabidopsis* seedling. Two-day-old *Arabidopsis* seedlings were hybridized with either (**A**) antisense or (**B**) sense strand specific *AUX1* digoxygenin-labeled RNA probes through use of a whole-mount in situ hybridization procedure (*33*). *AUX1* mRNA, visualized by strong purple coloration, is specifically localized within the root apex.

REFERENCES AND NOTES

1. M. Estelle, *Bioessays* **14**, 439 (1992).
2. J. Normanly, J. R. Cohen, G. R. Fink, *Proc. Natl. Acad. Sci. U.S.A.* **90**, 10355 (1993).
3. P. H. Rubery and A. R. Sheldrake, *Planta* **118**, 101 (1974).
4. D. L. Rayle and R. E. Cleland, *Plant Physiol.* **99**, 1271 (1992).
5. A. M. Jones, *Annu. Rev. Plant Physiol. Plant Mol. Biol.* **45**, 394 (1994).
6. H. M. O. Leyser *et al.*, *Nature* **364**, 161 (1993).
7. M. L. Evans, *Plant Physiol.* **95**, 1 (1991).
8. K. A. Feldmann, *Plant J.* **1**, 71 (1991).
9. E. P. Maher and S. J. B. Martindale, *Biochem. Genet.* **18**, 1041 (1980).
10. F. B. Pickett, A. K. Wilson, M. Estelle, *Plant Physiol.* **94**, 1462 (1990).
11. Root gravitropic curvature was measured in 30 to 40 4-day-old seedlings from each of the 6000 Arizona T-DNA lines as described [B. L. Bullen *et al.*, *Plant Physiol.* **93**, 525 (1990)]. One agravitropic mutant, *aux1-100*, was identified as being allelic with *aux1* when crossed with the *aux1-7* mutant (*10*).
12. Root thigmotropism was measured as described [K. Okada and Y. Shimura, *Science* **250**, 274 (1990)].
13. 2,4-D–sensitive root growth was measured as described in (*10*) to obtain median inhibitory concentration values of 4×10^{-7} M (*aux1-100*), 3.5×10^{-7} M (*aux1-7*), and 2×10^{-8} M [ecotype Wassilewskija (WS)].
14. To test for linkage between the T-DNA and *aux1-100* phenotype, we selfed 77 agravitropic progeny from a plant heterozygous for *aux1-100* and scored their progeny for kanamycin resistance. All of the progeny were kanamycin resistant, confirming that their agravitropic parents were homozygous for the T-DNA insert.
15. A 2.2-kbp fragment of plant-flanking DNA was plasmid rescued from *aux1-100* genomic DNA [as described in (*16*)]. Southern hybridization experiments with this radiolabeled fragment highlighted a Hind III RFLP between the wild-type (ecotype WS) and *aux1-100* DNA.
16. B. Schulz, M. J. Bennett, B. P. Dilkes, K. A. Feldmann, *Plant Molecular Biology Manual* K3 (Kluwer, Netherlands, 1994).
17. An *Arabidopsis* (ecotype WS) genomic library [as described in (*16*)] was screened with the radiolabeled 2.2-kbp fragment at high stringency [0.1 × standard saline citrate (SSC) and 0.1% SDS at 65°C] to isolate the homologous clone 20-1-1.
18. Mapping experiments with a recombinant inbred population [C. Lister and C. Dean, *Plant J.* **4**, 745 (1993)] concluded that a Dra I RFLP encoded by 20-1-1 was located on chromosome 2, close to the *AUX1* gene.
19. The PRL2 cDNA library [T. Newman *et al.*, *Plant Physiol.* **106**, 1241 (1994)] was screened at high stringency (0.1 × SSC and 0.1% SDS at 65°C) with a 20-1-1 probe, and multiple cDNA clones were characterized. A 5′ RACE (rapid amplification of cDNA ends) approach was used to confirm that the longest cDNA clone was full length.
20. EMBL accession number X98772.
21. Each *aux1* allele was isolated as three overlapping polymerase chain reaction fragments and then sequenced directly as described [S. Khorana, R. F. Gagel, G. J. Cote, *Nucl. Acids Res.* **22**, 3425 (1994)].
22. A 7.5-kbp Xho I–Bam HI fragment and a 4.4-kbp Eco RV–Bam HI fragment (Fig. 1) were subcloned into a Bin19-based kanamycin-resistant plant-transformation vector [M. Bevan, *Nucl. Acids Res.* **12**, 8711 (1984)]. The *XB7.5* and *EB4.4* constructs were transformed into the *aux1-7* mutant through use of a vacuum infiltration procedure [N. Bechtold *et al.*, *C. R. Acad. Sci. (Paris)* **316**, 1194 (1993)].
23. Restoration of auxin-sensitive root growth (*12*) and of gravitropic (*10*) and thigmotropic (*11*) bending responses were observed within the progeny of six independent *XB7.5* and *EB4.4* transformants.
24. Database searches were performed with the BLASTP program [S. F. Altschul *et al.*, *J. Mol. Biol.* **215**, 403 (1990)] at the National Center for Bioinformatics. Alignments were performed with the gap algorithm.
25. W. B. Frommer, S. Hummel, J. W. Reismeier, *Proc. Natl. Acad. Sci. U.S.A.* **90**, 5944 (1993); L. C. Hsu, T. J. Chiou, L. Chen, D. R. Bush, *ibid.*, p. 7441; M. Kwart, B. Hirner, S. Hummel, W. B. Frommer, *Plant J.* **4**, 993 (1993); W. N. Fischer, EMBL submissions S51168, S51169, and S51170; E. B. Lelanne, F. Vedel, R. DePaepe, EMBL submission U31932; D. Dillon and D. Stadler, *Genetics* **138**, 61 (1994).
26. *AUX1* transmembrane predictions were performed with software described by the following researchers: B. Rost *et al.*, *Protein Sci.* **4**, 521 (1994); M. Claros and G. von Heijne, *CABIOS* **10**, 685 (1994); D. M. Engelman, T. A. Steitz, A. Goldman, *Annu. Rev. Biophys. Biophys. Chem.* **15**, 321 (1986).
27. T. L. Lomax, G. K. Muday, P. Rubery, in *Plant Hormones and Their Role in Plant Growth and Development*, P. J. Davies, Ed. (Martinus Nijhoft, Dordrecht, ed. 2, 1994), pp. 509–530.
28. D. R. Bush, *Annu. Rev. Plant Physiol. Plant Mol. Biol.* **44**, 513 (1993).
29. T. L. Lomax and G. R. Hicks, *Biochem. Soc. Trans.* **20**, 64 (1992); R. Zettl *et al.*, *Proc. Natl. Acad. Sci. U.S.A.* **89**, 480 (1992).
30. G. K. Muday and P. Haworth, *Plant Physiol. Biochem.* **32**, 193 (1994).
31. S. Tsurumi and Y. Ohwaki, *Plant Cell Physiol.* **19**, 1195 (1978).
32. K. H. Hasenstein and M. L. Evans, *Plant Physiol.* **86**, 890 (1988).
33. A 350-bp fragment from the 5′ end of the *AUX1* cDNA was subcloned into the bluescript plasmid (Stratagene) and linearized with either Spe1 or Eco R1 in order to synthesize sense or antisense strand-specific *AUX1* RNA probes, respectively. The RNA probes were labeled with digoxygenin during in vitro transcription (Boehringer Mannheim) and then hydrolyzed to approximately 150 bases in length and then quantified; 10 ng of each probe were hybridized with 2-day-old *Arabidopsis* seedlings through use of a whole-mount in situ procedure [as described by D. Ludevid, H. Hofte, E. Himelblau, M. J. Chrispeels, *Plant Physiol.* **100**, 1633 (1992)].
34. S. Ward, A. Marchant, M. J. Bennett, unpublished data.
35. M. J. Vesper and C. L. Kuss, *Planta* **182**, 486 (1990).
36. M. L. Evans, H. Ishikawa, M. Estelle, *ibid.* **194**, 215 (1994).
37. S. T. May, A. Marchant, M. J. Bennett, unpublished data.
38. Abbreviations for the amino acid residues are as follows: A, Ala; C, Cys; D, Asp; E, Glu; F, Phe; G, Gly; H, His; I, Ile; K, Lys; L, Leu; M, Met; N, Asn; P, Pro; Q, Gln; R, Arg; S, Ser; T, Thr; V, Val; W, Trp; and Y, Tyr.

39. We thank S. C. Bennett, B. P. Dilkes, M. Schweigert, W. Woodward, and N. Forsthoefel for technical assistance. We thank M. Estelle for seeds of *aux1-7*, G. Roman and J. Ecker for seeds of *aux1-21* and *aux1-22*, N. Olszewski for the pOCA18 cosmid vector, and the *Arabidopsis* Biological Resource Center at Ohio State University for supplying the PRL2 cDNA library. Special thanks to M. Estelle, J. Digby, R. Firn, and G. Scherer for useful discussion. Supported by NATO (to M.J.B.), the Agricultural Food Research Council Plant Molecular Biology II/Biotechnology and Biological Sciences Research Council (to A.M., H.G.G., S.P.W., S.T.M., P.A.M., and A.R.W.), Deutsche Forschungsgemeinschaft (to B.S.), and NSF (to K.A.F.).

15 March 1996; accepted 1 July 1996